

1272471

RM-541

SOIL-TIRE MODEL FOR THE  
ANALYSIS OF OFF-ROAD  
TIRE PERFORMANCE

May 1972

RESEARCH DEPARTMENT

Best Available Copy

Reproduced by  
**NATIONAL TECHNICAL  
INFORMATION SERVICE**  
Springfield, Va. 22101

GRUMMAN AEROSPACE CORPORATION  
BETHPAGE NEW YORK

VH  
Grumman Research Department Memorandum RM-541

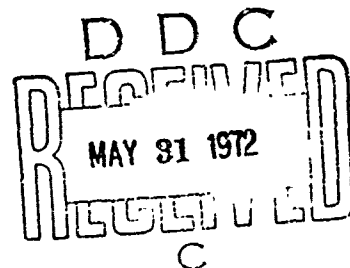
SOIL-TIRE MODEL FOR THE ANALYSIS OF  
OFF-ROAD TIRE PERFORMANCE

by

L. L. Karafiath

Materials and Structural Mechanics

May 1972



Approved by: *Charles E. Mack, Jr.*  
Charles E. Mack, Jr.  
Director of Research

DISTRIBUTION STATEMENT A  
Approved for public release;  
Distribution Unlimited

## DOCUMENT CONTROL DATA - R &amp; D

(Security classification of title, body of abstract and indexing annotation must be entered when the overall report is classified)

1. ORIGINATING ACTIVITY (Corporate author) Grumman Aerospace Corporation		2a. REPORT SECURITY CLASSIFICATION Unclassified	
		2b. GROUP n/a	
3. REPORT TITLE Soil-Tire Model for the Analysis of Off-Road Tire Performance			
4. DESCRIPTIVE NOTES (Type of report and inclusive dates) Research Memorandum			
5. AUTHOR(S) (First name, middle initial, last name) Leslie L. Karafiath			
6. REPORT DATE May 1972		7a. TOTAL NO. OF PAGES 25	7b. NO. OF REFS 20
8a. CONTRACT OR GRANT NO. none		8b. ORIGINATOR'S REPORT NUMBER(S) RM-541	
8c. PROJECT NO. c.		8d. OTHER REPORT NO(S) (Any other numbers that may be associated with this report) none	
8d.			
10. DISTRIBUTION STATEMENT Approved for public release; distribution unlimited			
11. SUPPLEMENTARY NOTES none		12. SPONSORING MILITARY ACTIVITY n/a	
13. ABSTRACT The analysis of off-road tire performance by rigid wheel models yields acceptable results only when the tire is stiff relative to the soil. In cases where the tire stiffness is low relative to the ground it is necessary to consider the effect of tire deformation on soil-tire interaction. A study of available experimental data showed that tire deformation limits the maximum pressure that can develop in the soil under the tire load. On this basis a soil-tire model has been developed that takes the effects of tire deflection into account. Failure conditions in the soil govern the interface stresses where these do not exceed a limit pressure established on the basis of tire deflection; the interface stresses are calculated with consideration of the deflected tire geometry. In the center flat portion of the tire where hypothetical soil pressure calculated from soil failure conditions would exceed the limit, the pressure is assumed to equal the limit pressure. Sample computations show good agreement with experimental results in regard to tire deflection and performance characteristics.			

14.	KEY WORDS	LINK A		LINK B		LINK C	
		ROLE	WT	ROLE	WT	ROLE	WT
	Rigid Wheel Models Tire Deformation Tire Deflection Interface Stresses						

### ABSTRACT

The analysis of off-road tire performance by rigid wheel models yields acceptable results only when the tire is stiff relative to the soil. In cases where the tire stiffness is low relative to the ground it is necessary to consider the effect of tire deformation on soil-tire interaction. A study of available experimental data showed that tire deformation limits the maximum pressure that can develop in the soil under the tire load. On this basis a soil-tire model has been developed that takes the effects of tire deflection into account. Failure conditions in the soil govern the interface stresses where these do not exceed a limit pressure established on the basis of tire deflection; the interface stresses are calculated with consideration of the deflected tire geometry. In the center flat portion of the tire where hypothetical soil pressure calculated from soil failure conditions would exceed the limit, the pressure is assumed to equal the limit pressure. Sample computations show good agreement with experimental results in regard to tire deflection and performance characteristics.

## TABLE OF CONTENTS

<u>Item</u>	<u>Page</u>
Introduction .....	1
Deformation of Tires on Rigid Surfaces and in Yielding Soils .....	2
Stresses at the Soil-Tire Interface .....	6
Soil-Tire Model .....	11
General Considerations .....	11
Effect of Soil Properties .....	13
Model Description .....	13
Application of the Soil-Tire Model for Tire Performance Computations .....	17
Conclusions and Recommendations .....	23
References .....	24

## LIST OF ILLUSTRATIONS

<u>Figure</u>		<u>Page</u>
1	Pneumatic Tire Terms .....	3
2	Centerline Deflections of a 9.00-14 Tire Under Various Loading Conditions (from Ref. 9) .....	5
3	Contour Maps of Pressure Distribution Under 11-38 Smooth Tire on Firm Sand (from Ref. 14) .....	8
4	Vertical Components of Normal Stresses Measured in Sand (from Ref. 15) .....	9
5	Distribution of Normal and Tangential Stresses Beneath Tire (a) and Rigid Wheel (b) in Sandy Loam. Tire deflection not shown (from Ref. 10) .....	10
6	Soil-Tire Model .....	14
7	General Pattern of Interface Stress Distribution in a Soil-Tire Model .....	16
8	Shape of the Soil-Tire Model with Outlines of Failure Zones and Computed Interface Stresses .....	20
9	Slip Line Field Computed for the Rear Field of Case b) Shown by Outline in Fig. 8 .....	21

## LIST OF SYMBOLS

$c$	= cohesion
$CI$	= cone index
$p$	= average pressure
$p_c$	= equivalent carcass pressure
$p_i$	= inflation pressure
$p_l$	= limit normal stress
$r$	= deflected radius
$R$	= undeflected radius
$x, z$	= coordinates
$\alpha$	= central angle
$\alpha', \alpha''$	= angles defining start and end of deflection
$\alpha_e$	= entry angle
$\alpha_d, \alpha'_d$	= angle defining ends of flat portion
$\alpha_r$	= rear angle
$\beta$	= constant in Eq. (2)
$\gamma$	= unit weight of soil
$\delta$	= angle of inclination of resultant stress to normal
$\Delta$	= deflection
$\epsilon$	= slope angle
$\phi$	= friction angle
$\theta$	= angle enclosed by major principal stress and $x$ axis



$\mu$             =  $45^\circ - \phi/2$   
 $\sigma_n$         = normal stress  
 $\sigma_{1,2,3}$     = principal stresses  
 $\sigma$            =  $\frac{1}{2}(\sigma_1 + \sigma_3)$   
 $\tau$             = shear stress

**THIS  
PAGE  
IS  
MISSING  
IN  
ORIGINAL  
DOCUMENT**

## DEFORMATION OF TIRES ON RIGID SURFACES AND IN YIELDING SOILS

A measure of the deformation of tires is the shape and size of the contact area. On rigid surfaces, tire deflection defines the contact area and, thereby, the intensity of the ground pressure under tire loads. The contact area of tires may be approximated by a rectangle, an ellipse, or a torus section; for these shapes, relationships between deflection and contact area have been derived for various inflation pressures (Ref. 4). From the viewpoint of soil-tire interaction, the significance of contact area determinations on rigid surfaces is that it establishes a lower limit for the contact area in yielding soils.

The deflection of a tire on a rigid surface ( $\Delta$ ) is defined as the difference between unloaded and loaded section height (Fig. 1), and percentage deflection ( $100 \cdot \Delta/h$ ) as the percentile ratio of the deflection to the section height. This measure of tire flexibility was introduced by the U.S. Army Corps of Engineers Waterways Experiment Station (WES), in its dimensional analysis of tire performance as a tire deformation characteristic (Ref. 5).

While the deflection of the tire on a rigid surface is a useful empirical measure of tire flexibility, it does not allow the calculation of tire deflection under other than vertical loads or on yielding surfaces. For the computation of the deformation of a tire rolling on a rigid surface, a tire model consisting of a cylindrical shell has been developed (Refs. 6, 7). The inflation pressure is modeled by springs acting on the cylindrical shell from the inside. For the analysis of stresses and strains induced in the tire carcass by the inflation pressure, another model consisting of a shell of revolution has been proposed (Ref. 8). Although deformation of the tire under the conditions for which the model was developed is reasonably approximated by these models, the elastic and other constants used in the models are generally not available for tires. Computation of tire deformation on a yielding surface using the cylindrical shell model would be possible only if the response of the yielding surface were adequately represented by a spring model. This is not the case with soils in failure condition when interacting with wheels or tires.

Measurements of tire deformation in yielding soils have been undertaken by several investigators. Freitag and Smith (Ref. 9)

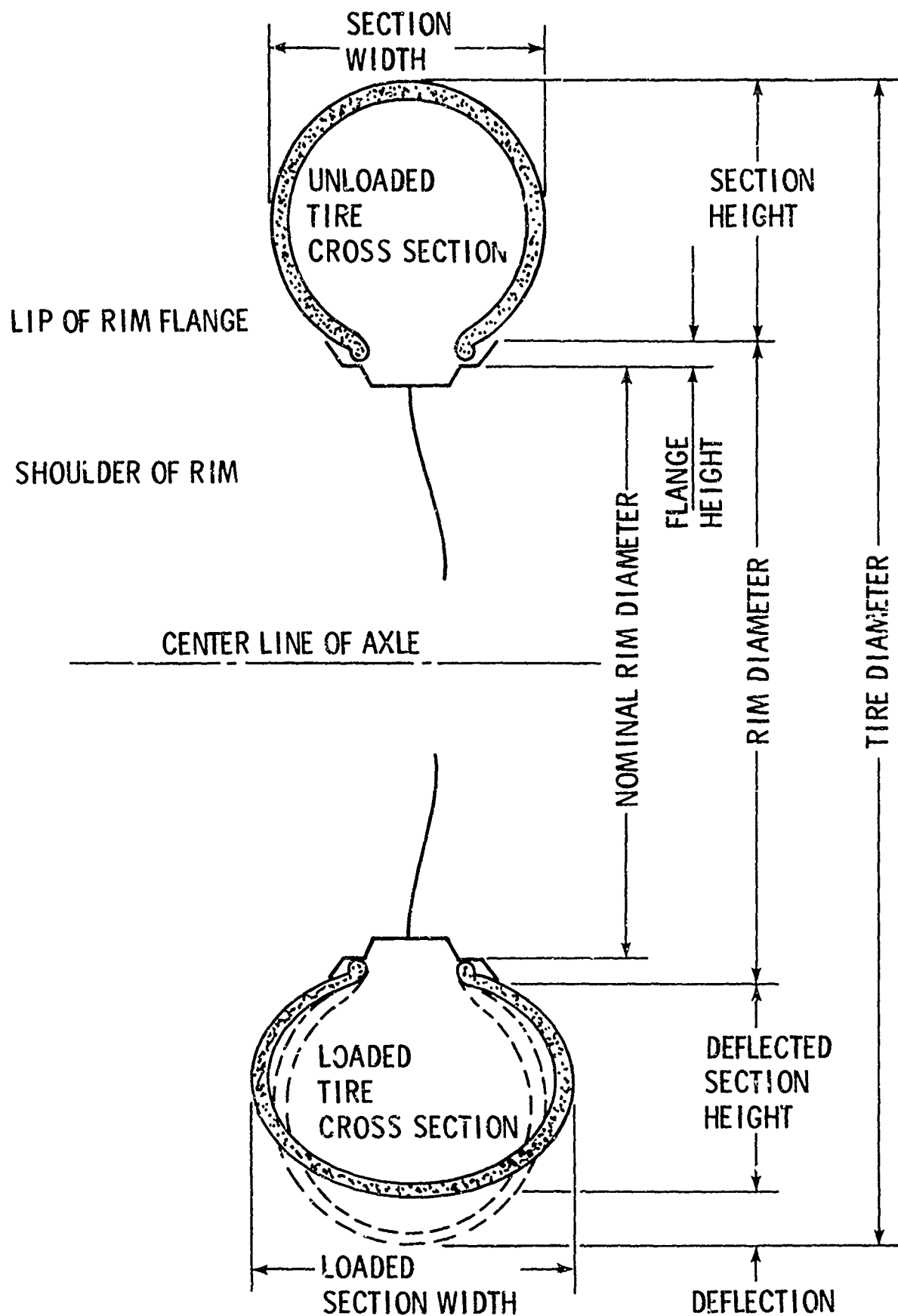
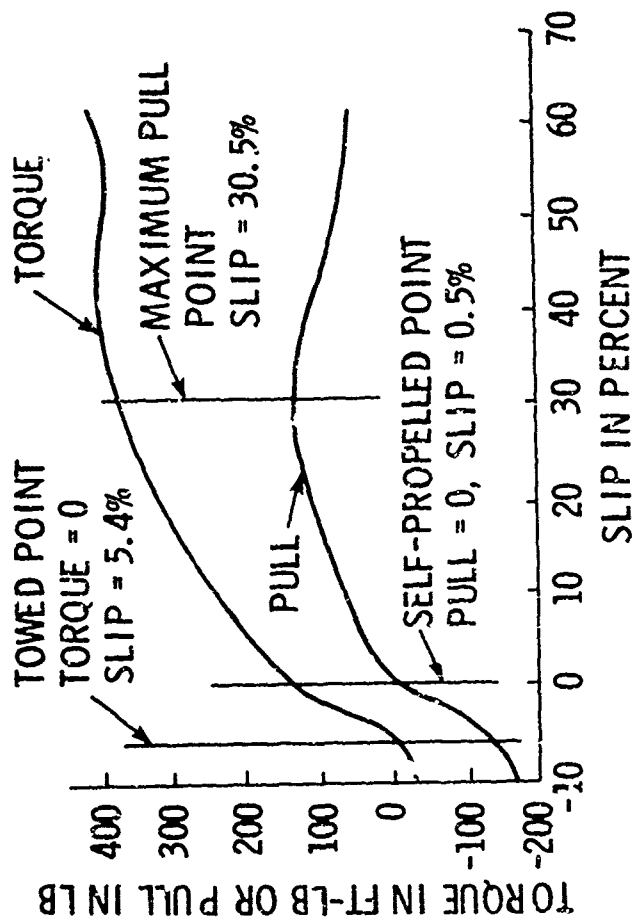


Fig. 1 Pneumatic Tire Terms (from Ref. 5)

presented a comprehensive evaluation of centerline deflections of tires measured under a variety of soil strength, inflation pressure, and loading and slip conditions. A typical result of their investigations is shown in Fig. 2 where centerline deflections of a 9.00-14 tire in Yuma sand are shown for various percentages of slip. With increasing slip, higher and higher shear stresses are transmitted to the soil at the soil-tire interface. These shear stresses decrease the capacity of soil to carry loads. The stiffness of the tire relative to the ground increases with increasing slip and the tire shape approaches that of a rigid wheel. Other results presented in Ref. 9 point to the same qualitative conclusion: the shape of the deflected tire depends on the stiffness of the tire relative to that of the ground. Other deflection and tire imprint measurements (Refs. 10, 11) generally confirm the above conclusions.



TEST CONDITIONS  
 9.00-14, 2-PR TIRE  
 12.5-PSI INFLATION PRESSURE  
 600-LB LOAD, 35% DEFLECTION  
 25 CONE INDEX  
 FIRST PASS, YUMA SAND

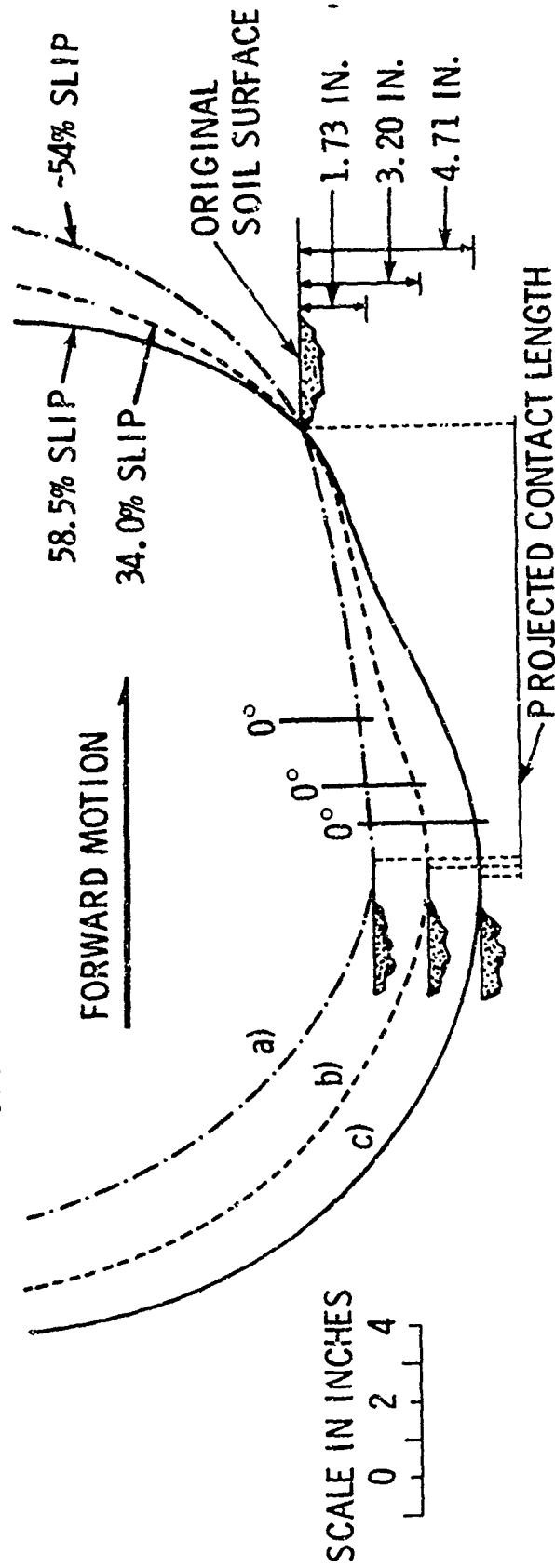


Fig. 2 Centerline Deflections of a 9.00-14 Tire Under Various Loading Conditions (from Ref. 9)

## STRESSES AT THE SOIL-TIRE INTERFACE

Tire deformation affects soil-tire interaction in two ways: it changes the geometry of the soil-tire interface, and it relieves the stresses that would develop in the soil if the interface were undeformable. Stress measurements at the soil-tire interface confirm this latter effect and give an indication of the magnitude of stress relief.

The interface stresses generated by the tire load on a given surface are influenced not only by the size and shape of the tire and the applied inflation pressure, but also by the type of tire construction, and the geometry and properties of the tread. To eliminate variations in stresses due to differences in the tread, tests conducted at WES were generally performed with treadless or buffed tires. Other experimenters used heavily lugged tractor tires to determine the effect of these lugs on the pattern of stress distribution. Even though a considerable number of experiments were performed for the purpose of interface stress measurements, only very general conclusions can be drawn because of the wide variety of tires as well as soil conditions.

At WES, tire interface stress measurements were first made on unyielding surfaces that allowed the placement of the sensors in the unyielding surface rather than in the tire (Ref. 12). Results of these measurements are of interest for soil-tire interaction studies because stresses measured on an unyielding surface represent the upper limit of stresses that would develop in a soil that yields relatively little under the tire load. Measurements of normal stresses in the contact area of stationary and slowly rolling tires were conducted at WES in 1961 as a first step in gaining information on the nature of pressure distribution at the soil-tire interface. The general pattern of stress distribution observed in these tests showed a center portion in the contact area with fairly uniform stress distribution and stress concentrations called "edge stresses" at the perimeter of the contact area. These edge stresses are related to the sidewall stiffness of the tire while the magnitude of the average center portion stresses is related to the inflation pressure of the tire. Experiments performed at the Munich Polytechnic (Ref. 13) generally confirmed the above findings.

Measurements of interface stresses in soils were made by VandenBerg and Gill (Ref. 14). These measurements, using smooth

tires, indicate a stress distribution pattern similar to that observed on unyielding surfaces (Fig. 3). The magnitude of the uniform pressure in the center portion depends on the inflation pressure and is generally somewhat higher.

Freitag et al. (Ref. 15) investigated the distribution of normal stresses in the contact area of both towed and powered tires inflated to various pressures. Tests were carried out in both sand and clay. A typical result of these measurements is indicated in Fig. 4. The vertical components of the normal stresses measured in the centerline and 3.75 inches off-center of a 11.0-20 tire, inflated to 19 psi are shown for powered and towed condition. The maximum stress in each case exceeds only slightly the inflation pressure. The resultant of the normal stresses in all of the 32 tests performed passed within 0.5 inch of the axle centerline, indicating that tire deflections were such that normal stresses did not generate any torque, a condition that is characteristic of rigid wheels.

Krick (Ref. 10) also measured both normal and shear stresses on the interface of both rigid wheels and tires in a sandy loam. Figure 5 shows the result of one of one of his measurements, referenced to the undeflected tire, obtained at 40 percent slip. The effect of tire deflection on restraining the maximum normal stress is evident if normal stresses measured on tires are compared with those measured on rigid wheels under the same loading conditions.

Trabbic et al. (Ref. 16) measured soil-tire interface pressures on the undertread, lug face, and trailing lug side of tractor tires at various drawbar loads and tire inflation pressures. Stress concentration on the lug faces as opposed to the undertread was observed. The general trend of the effect of tire inflation pressure confirmed the previous findings.



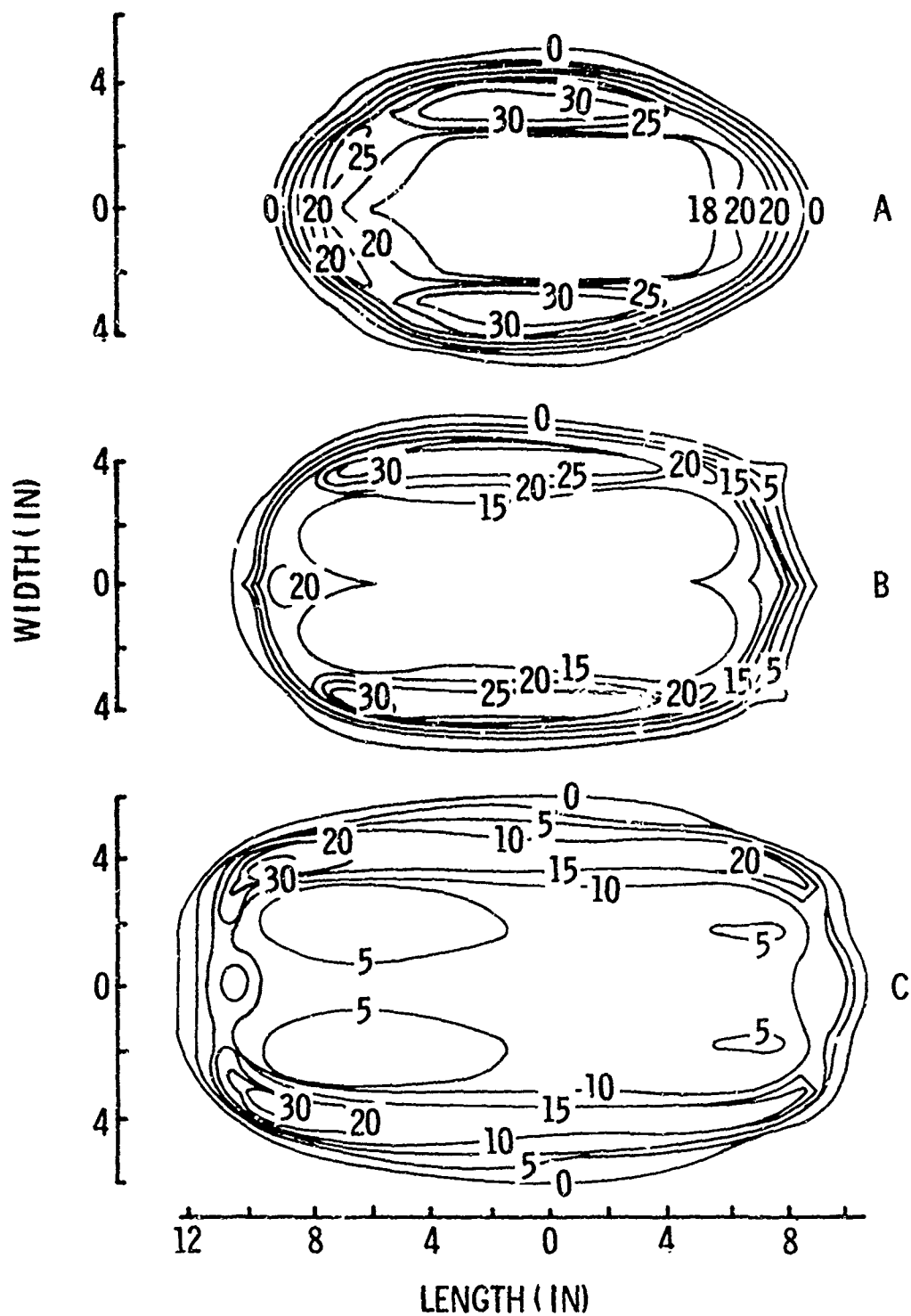
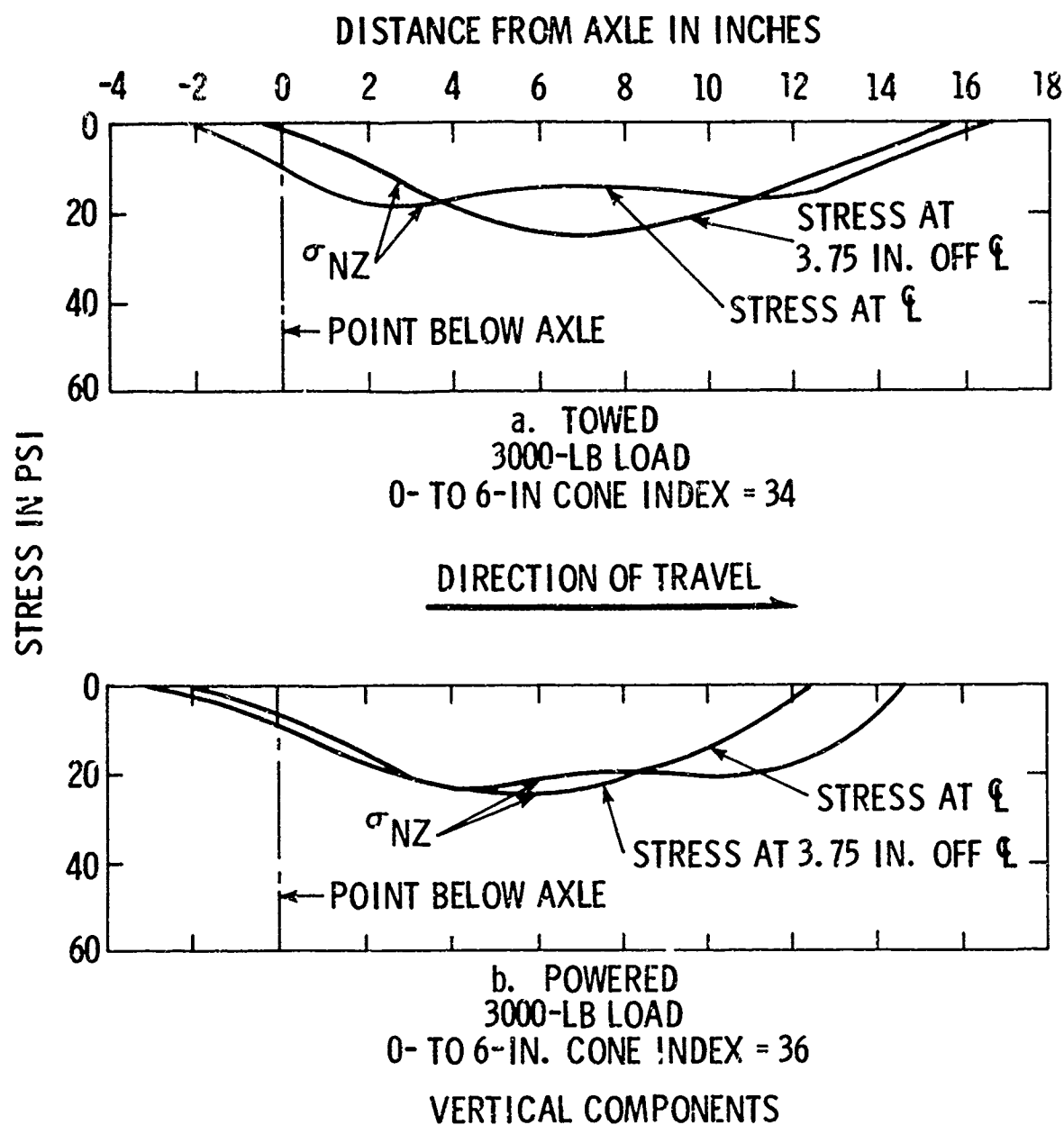
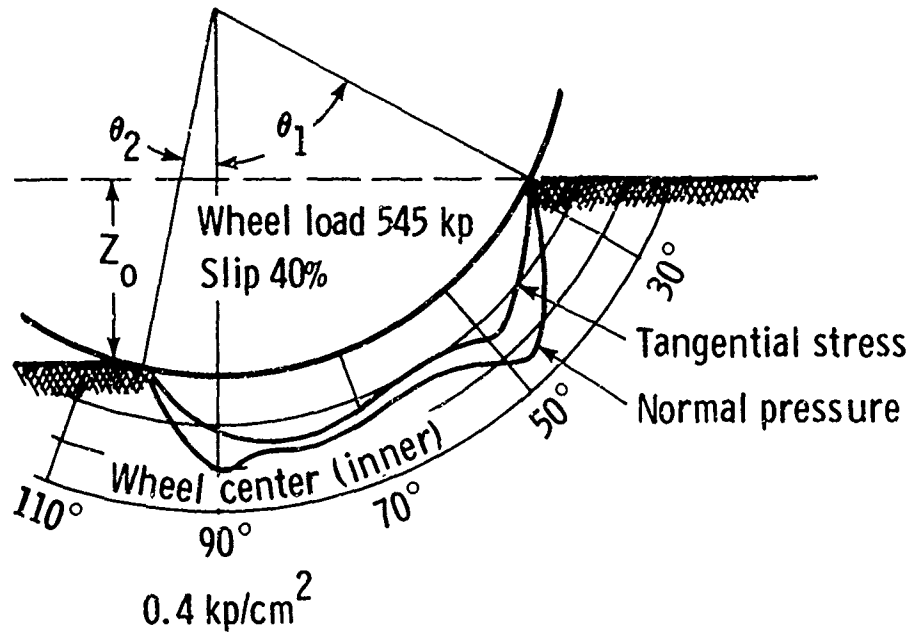


Fig. 3 Contour Maps of Pressure Distribution Under 11-38 Smooth Tire on Firm Sand Inflated to: (A) 14 psi; (B) 10 psi; (C) 6 psi. The direction of travel of the tire was from right to left. Numbers indicate pressure in psi (from Ref. 14)

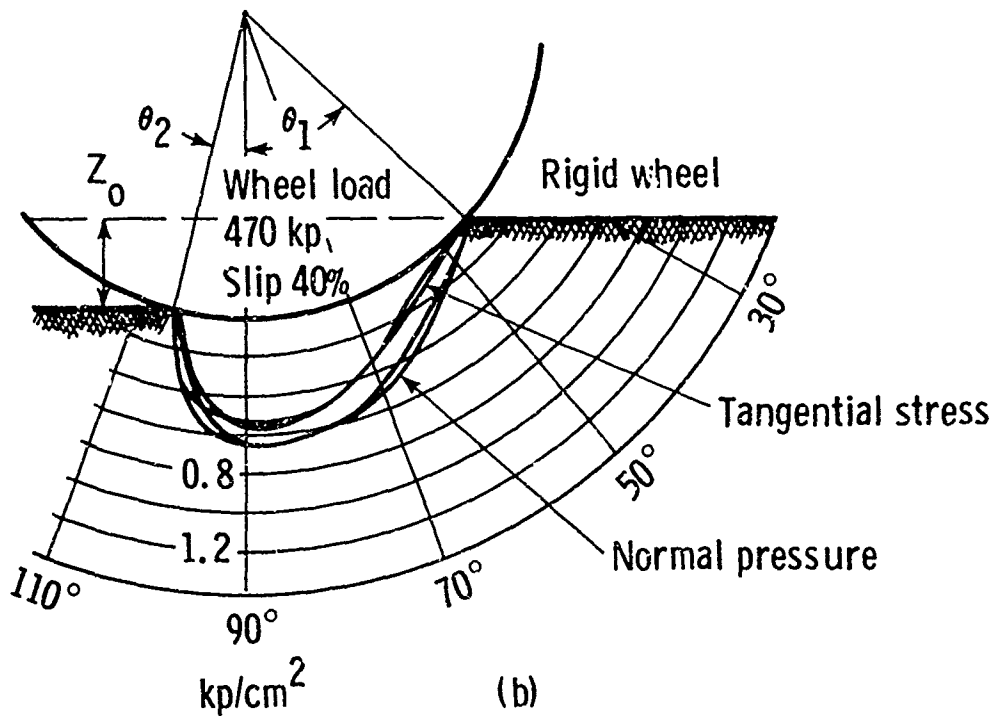


TOWED AND POWERED WHEELS  
11.00-20, 12-PR SMOOTH TIRE  
19-PSI INFLATION PRESSURE

Fig. 4 Vertical Components of Normal Stresses  
Measured in Sand (from Ref. 17)



(a)



(b)

Fig. 5 Distribution of Normal and Tangential Stresses Beneath Tire (a) and Rigid Wheel (b) in Sandy Loam. Tire deflection not shown (from Ref. 10).

## SOIL-TIRE MODEL

### General Considerations

The deformation and stress measurements discussed briefly in the preceding paragraphs indicate the complexity of the soil-tire interaction problem. The shape of the tire and geometry of the contact area depend not only on the properties of the tire, but on the properties of soil and on the loads applied. The stresses measured in the contact area are far from uniform. Stress concentrations occur at the edges of the contact area. Obviously, all these variations cannot be considered in any workable soil-tire model and simplifications are required. An appropriately simplified model often yields sufficiently accurate results, as many computational methods in engineering demonstrate.

To decide what simplifications can be undertaken in a model without jeopardizing its accuracy and usefulness, it is expedient to consider the tire as a free body and to assess the effect of possible simplifications on the performance of the tire. The edge stresses in the contact area, as experiments indicate, are symmetrical both crosswise and lengthwise. This symmetry allows one to consider average stresses across the tire width without any significant loss of accuracy. Likewise, edge stresses may be smoothed lengthwise and the resulting torque, load, and drawbar pull still may be reasonably close to the actual values. Conversely, it is important to duplicate the deflected shape of the tire and its orientation to the ground surface as closely as possible. In the summation of the interface stresses for the computation of drawbar pull, the inclination of interface elements relative to the ground surface cannot be neglected. Depending on the inclination of the element, normal stresses on the interface yield a component (plus or minus) in the direction of the drawbar pull that may or may not be significant relative to the component of shear stresses.

To treat the soil-tire interaction two dimensionally, it is necessary to assume that the width of the contact area is constant. This assumption is reasonable for certain types of tires; for others it may be necessary to allow a change of the width of the tire with the loading conditions. In this Memorandum, only the former case is considered.

The effect of tire deformation on soil reaction is another important factor that has to be considered in a soil-tire model. Soil

reaction stresses on rigid wheels are controlled by the failure conditions in the soil that develop beneath towed or driven rigid wheels under the applied wheel load (Refs. 1, 2). In the case of rigid wheels, there is no limit to the interface stresses other than that imposed by soil failure criteria. Experiments with tires indicate that except for local stress concentrations, tire deformation does not allow the development of stresses higher than a certain limit normal stress ( $p_1$ ). However, that depends on the inflation pressure. In this respect, it is of interest to review the data on the average contact stresses obtained with stationary and rolling tires on a rigid surface and the relationships proposed to relate these average contact stresses to inflation pressure. Since the contact area in yielding soils is always greater than on a rigid surface, the average stresses for the same load are lower than those obtained on a rigid surface. Thus, the average stresses measured on the rigid surfaces represent an upper limit to the average stresses in yielding soils.

The general form of the equations proposed by various researchers for the relationship between average contact stress and inflation pressure is as follows:

$$p = c_1 p_i + p_c \quad (1)$$

where

$p$  = average contact stress

$p_i$  = inflation pressure

$p_c$  = pressure due to the carcass stiffness

$c_1$  = constant .

Bekker and Janosi (Ref. 17) found that  $p_c$  was independent of the inflation pressure and concluded that it equally applies for yielding and unyielding surfaces. For a 7.00 x 16 tire,  $p_c$  was found to vary from 2.4 psi for a 200-pound load to 4.8 psi for 700 pounds with  $c_1 = 1$ . Other experiments performed to determine the contact pressure beneath tires of earth compacting equipment (Ref. 18) indicate that  $c_1$  may be as low as 0.6 for high inflation pressures. Ageikin (Ref. 19) suggested a value varying from 0.9 to 1.0 for  $c_1$  and 6 to 10 psi for  $p_c$ ; in his notation, however,  $p$  is the mean pressure in the flattened portion of the tire and not the average pressure over the whole contact area.

## Effect of Soil Properties

The preceding discussion centered around the effect of tire deformation on the distribution and summation of stresses. While tire deflection limits the stresses in the center portion of the contact area, soil properties impose another limitation to the rise and fall of the stresses along the wheel perimeter. For the deflected shape of the tire, the limit interface stresses, controlled by failure conditions in the soil, can be established the same way as for rigid wheels (Refs. 1, 2). The limits imposed on the interface stresses by the properties of soil will govern whenever these stresses are lower than that would develop on a rigid surface. However, soil properties cease to govern when interface stresses computed on the basis of soil failure conditions exceed the limit imposed on the stresses by the flexibility of tires.

## Model Description

A soil-tire model that allows the consideration of all essential factors affecting tire performance is presented below. The tire is assumed to have a constant width both in the undeformed and in the deformed state. The stresses across the tire width are assumed to be uniform so that the soil-tire interaction problem can be treated as two dimensional. Tire deformation is represented by the shape of the tire in the center plane in the direction of travel. Tire shape is assumed to be the same in all parallel planes. The deformation is assumed to consist of two curvilinear segments separated by a linear or flat section (Fig. 6). It is assumed that the tire starts to deform an angle  $\alpha'$  ahead of the entry angle ( $\alpha_e$ ) and reaches its original form an angle  $\alpha''$  past the exit angle  $\alpha_r$ . In the front curvilinear segment, the radii decrease according to the following relationship:

$$r = R e^{\beta(\alpha - \alpha_e - \alpha')} \quad (2)$$

where

$R$  = radius of unloaded tire

$r$  = deflected radius

$\beta$  = constant .

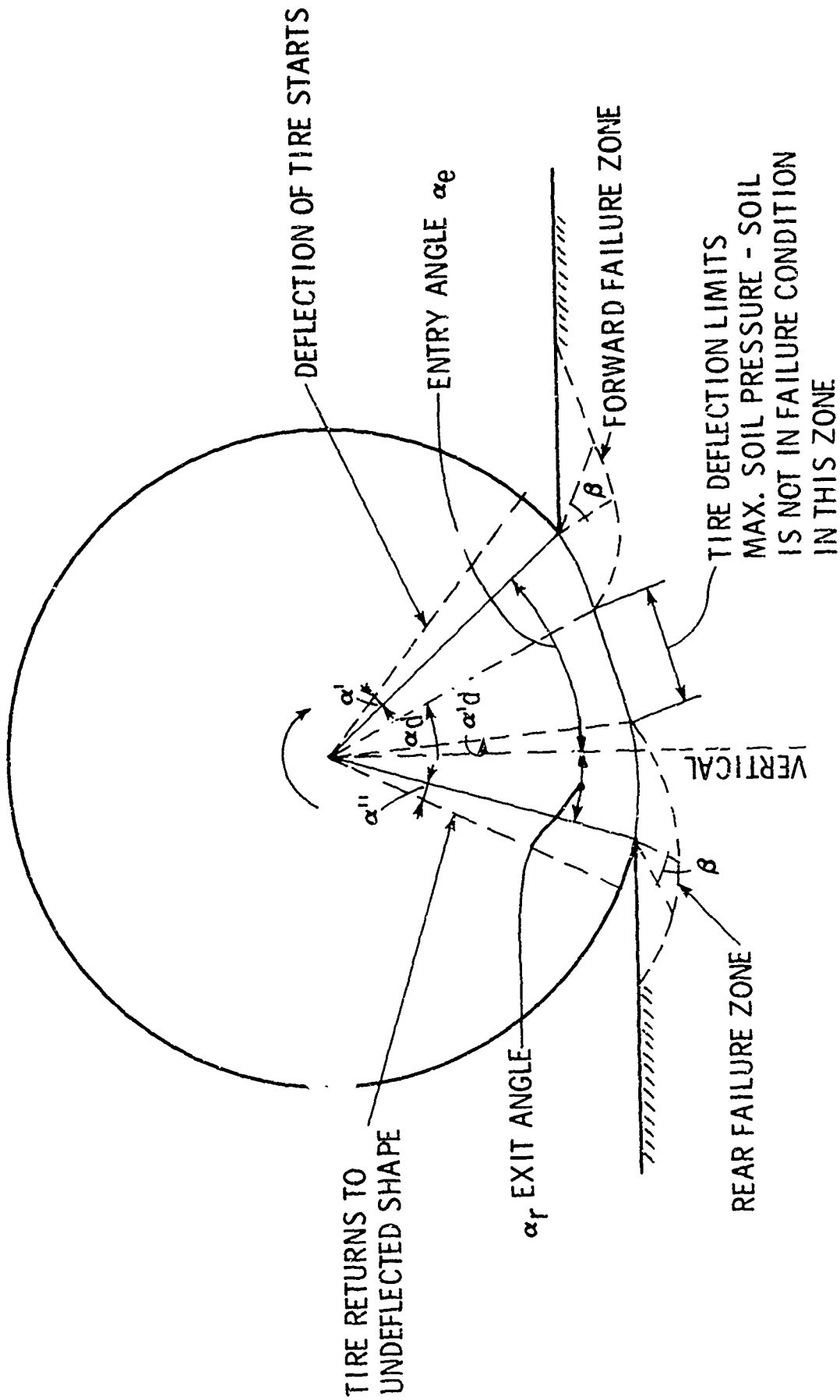


Fig. 6 Soil-Tire Model

In the rear curvilinear segment, the radii decrease according the same type of relationship. The constant  $\beta$  is computed from deflection  $\Delta$  at  $\alpha_d$  where  $r = R - \Delta$  as follows:

$$\beta = \frac{\log (1 - \Delta)}{\alpha_d - \alpha_e - \alpha} \quad (3)$$

where  $\alpha_d$  = angle defining the front end of flat portion. In the flat portion, it is assumed that the normal stress equals the limit,  $p_1$ , and the angles  $\alpha_d$ ,  $\alpha'_d$  are determined from this condition by calculating the normal stresses from the failure conditions in the soil in the front and rear slip line fields, respectively.

The interface stresses between the entry angle,  $\alpha_e$  and  $\alpha'_d$ , as well as those between the exit angle,  $\alpha_r$ , and  $\alpha_d$ , are assumed to be controlled by failure conditions in the soil. Outlines of the respective slip line fields are shown by dashed lines in Fig. 6. The geometry of these failure zones and the associated stresses are computed the same way as described for rigid wheels in Fig. 1 and Fig. 2; however the deflected geometry of the tire at the interface, as defined by Eq. (2), is considered. Generally, deflection of the tire influences the interface stresses favorably because the central angle of the radial shear zone ( $\beta$  in Fig. 5) is larger with the deformed than the undeformed shape. The radial shear zone is the "seat" of stress increases in the failure zone, as theory and computations show.

In the case of strong soils, the extent of the front and/or rear failure zone may diminish or even vanish. In this case, the tire may be considered as rolling on a rigid surface.

As in the case of rigid wheels, the geometry of the failure zones and the associated stresses are to a great degree dependent on the shear stress developing with slip at the interface. The effect of interface stresses on the shape of the tire and performance parameters is shown by an example in the following section.

The general shape of the shear and normal stress distribution curves obtained with the soil-tire model is shown in Fig. 7. A comparison of this shape with those shown in Fig. 4 indicates that the soil-tire model is suitable qualitatively for the approximation of experimental stress distribution curves. Quantitative comparisons with experimental data are given in the next section.





## APPLICATION OF THE SOIL-TIRE MODEL FOR TIRE PERFORMANCE COMPUTATIONS

The soil-tire model presented in the preceding section is amenable to tire performance calculations by computer. The basis of tire performance calculation is the determination of interface stresses and their appropriate integration to yield the values of load, torque, and drawbar pull characteristic of tire performance. The normal stress in the flattened portion of the tire equals the pressure,  $p_1$ . In the curved front and rear zones, the interface stresses are determined by failure conditions in the soil. These are governed by differential equations of plasticity as follows (Ref. 1):

$$dz = dx \tan(\theta \pm \mu)$$

$$d\sigma \pm 2\sigma \tan \phi d\theta = \frac{\gamma}{\cos \phi} [\sin(\epsilon \pm \phi) dx + \cos(\epsilon \pm \phi) dz] \quad (4)$$

The numerical integration of the above differential equations yields the geometry of the slip line field and the associated stresses for the boundary conditions defined by the tire geometry and interface friction. Solution procedures for either of the slip line fields of the soil-tire model shown in Fig. 6 are essentially the same as for the slip line fields beneath rigid wheels described in detail in Refs. 1 and 2 and those, for the sake of brevity, are not discussed here. One minor difference in the computation is that the geometry of the interface boundary is no longer circular, but corresponds to the deflected shape of the tire.

In the soil-tire model, the extent of the front and rear slip line fields is determined by the condition that the normal stress may not exceed  $p_1$ , the average stress in the flat portion of the tire. For this condition and a given interface friction, the slip line field geometry and the interface stresses are uniquely determined. The interface friction is assumed to be uniform over the whole interface. In the integration of interface stresses, the deflected shape of the tire is considered. Since the interface elements are generally not perpendicular to the radii, the torque component of normal stresses on an element is not per se zero, as it is in the case of rigid wheels. However, a number of shape and

slip line field determinations for soil-tire models performed for various conditions in the course of the model development showed that the total torque due to normal stresses is always negligible. This finding is consistent with the empirical criterion for tire shape deformation established by Freitag et al. in Ref. 9.

To illustrate that the proposed soil-tire model is a working model suitable to duplicate tire behavior, tentative computations were made for the conditions of tire deflection and performance measurements reported in Ref. 9, and are shown in Fig. 2.

The following conditions were established for use in the soil-tire model:

- **Soil Properties.** The experiments were performed in Yuma sand at a density corresponding to a cone index (CI) of 25. Assuming that this CI represents the average reading in the upper 6-inch layer, the cone index gradient (G) equals 8.33 psi/in. ( $2.26 \text{ MN/m}^3$ ), corresponding to a relative density of about 72 percent (Ref. 20). For this density, the friction angle of the Yuma sand, as determined by triaxial tests, can be assumed as 39 degrees (Fig. B-10 in Ref. 20). Beneath the rear field, however, the sand is considerably compacted and its friction angle was assumed as  $40^\circ$ ,  $42^\circ$ , and  $43^\circ$ , respectively, for cases a), b), and c) in Fig. 2. The unit weight of the sand was assumed as  $100 \text{ lbs/ft}^3$  in the front and as  $110 \text{ lbs/ft}^3$  in the rear zone.
- **Tire Properties.** The deflection of the tire on a rigid surface is given as 35 percent of the height of the section (6.4 inches), which corresponds to about 2.15 inches or 15 percent shortening of the nominal tire radius. In yielding soils, tire deflection is less than that obtained on a rigid surface. In the soil-tire model, shortening of the radius at angle  $\alpha_d$  was assumed as 6 percent, resulting in a maximum shortening at the center of the flat portion of 8, 7, and 6 percent, respectively, in cases a, b, and c.

In the test series shown in Fig. 2, no interface stress measurements were made. The value of the limiting normal pressure had to be estimated on the basis of information available from tests performed elsewhere. For the inflation pressure of 12.5 psi of the test series,  $p_1$  was estimated as 14 psi.

In the model, the following nominal dimensions were used for the 9.00-14 tire:

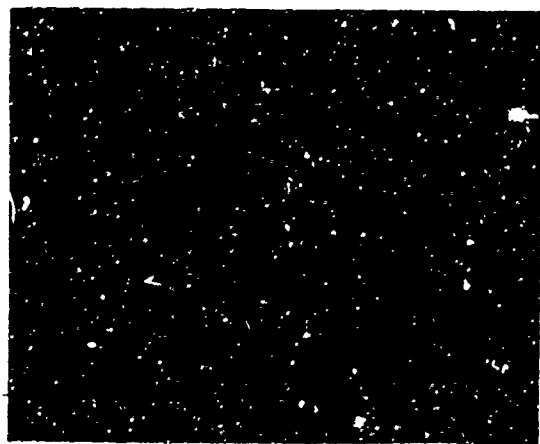
Undelected radius       $R = 1.18 \text{ ft}$

Width                       $b = 0.69 \text{ ft}$

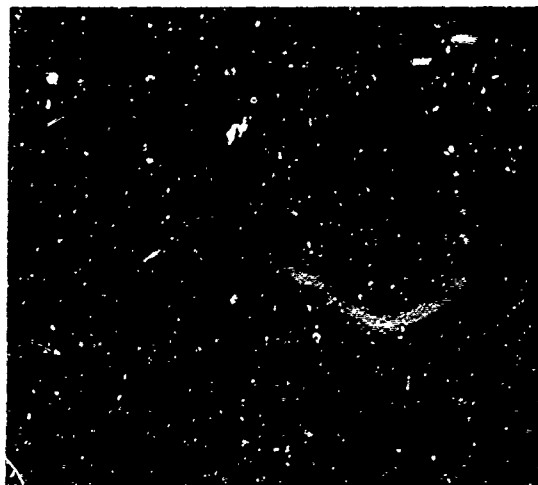
- Interface friction. In the experiments, interface friction was not measured. For the three cases shown in Fig. 2, interface friction angles of  $\delta = 0, 20.5^\circ$ , and  $26.5^\circ$  yielded reasonably good approximations of the measured load, torque and drawbar pull values at -5.4, 34, and 58.5 percent slip. Unfortunately, relationships that connect interface friction values with slip have not yet been sufficiently validated, even for rigid wheels. For tires, this problem is complicated by the relatively large deformation of the tire material. The hysteresis in rubber deformation results in slip phenomena even on rigid surfaces. The evaluation of the relative displacement between tire surface and soil is extremely difficult. Further research is needed to establish slip-interface friction relationships for tires.

Figure 8 shows the tire shapes as well as the outlines of the slip line fields obtained by the computer program and displayed on a visual display terminal. These results were obtained with the above soil-tire model for the experimental conditions shown in Fig. 2. A slip line field, as determined computationally, is shown in detail in Fig. 9 for the rear field of case b shown in Fig. 8. The computed normal and shear stresses are also shown in Fig. 8 below each figure for developed central angles. The normal stress under the flat portion of the tire was allowed to vary slightly from the front field to the rear field to reduce computer time required for the exact matching of stresses. The tire performance characteristics obtained with the model shown in Fig. 6, together with those measured in the experiments, are tabulated in Table 1.

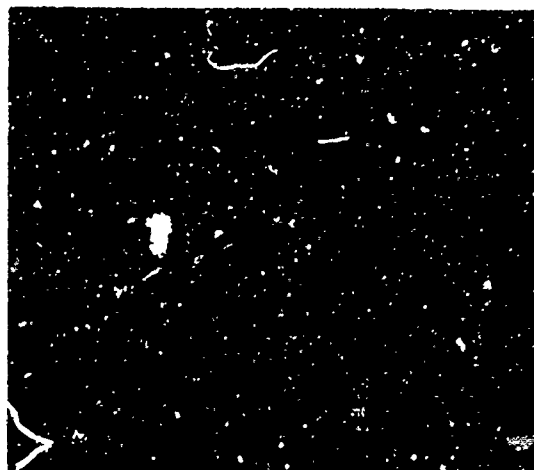
It is seen that the measured tire performance characteristics are reasonably well duplicated by the computations. The range of deviations is about the same magnitude as the range of accuracy within which this type of experiment is repeatable.



(a)



(b)



(c)

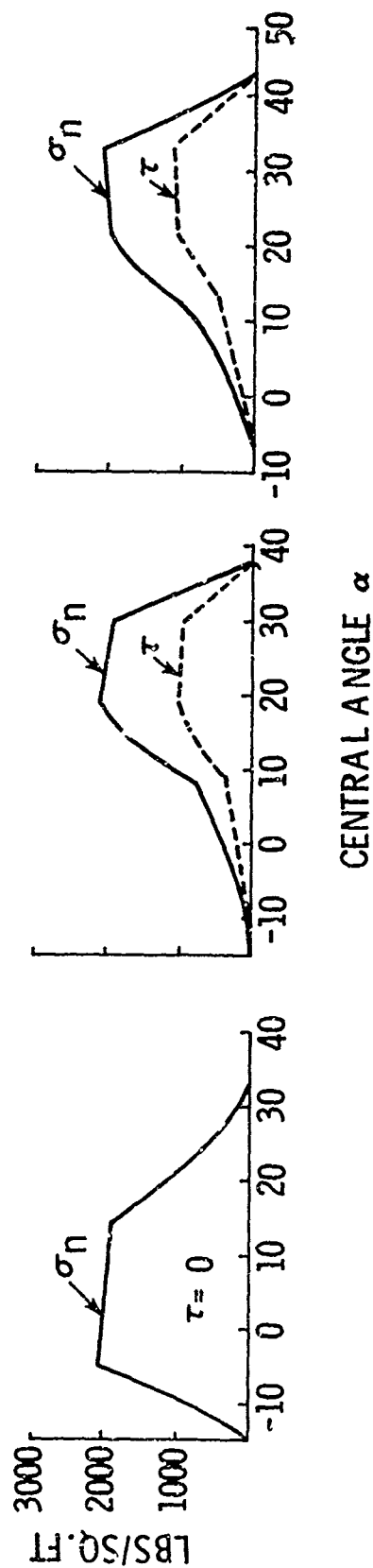


Fig. 8 Shape of the Soil-Tire Model with Outlines of Failure Zones and Computed Interface Stresses

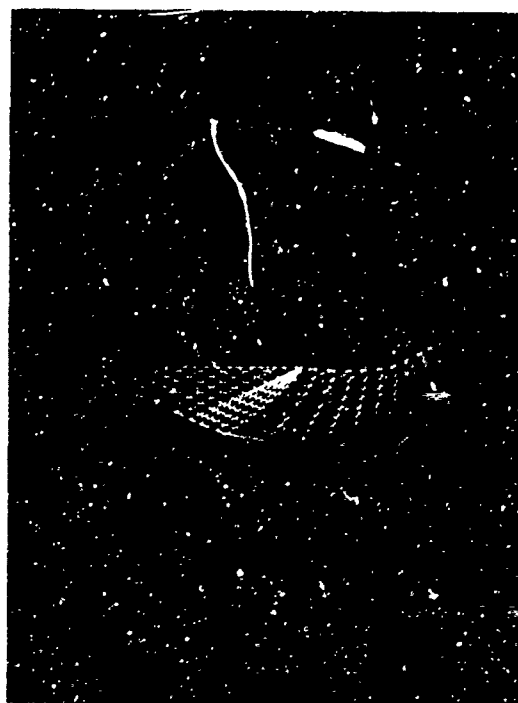


Fig. 9 Slip Line Field Computed for the Rear Field  
of Case (b) Shown by Outline in Fig. 8

Table 1

COMPARISON OF MEASURED AND COMPUTED PERFORMANCE CHARACTERISTICS

		Case		
		a	b	c
Slip %	Measured	- 5.4	34	58.5
	Assumed	0	26.5	27.5
Load (lbs)	Measured	860	860	860
	Computed	837	874	849
Torque (ft-lb)	Measured	0	390	420
	Computed	- 0.3	425	442
Drawbar Pull (lbs)	Measured	-140	130	70
	Computed	- 96	1'5	84
Sinkage (in.)	Measured	1.79	3.20	4.71
	Computed	1.79	2.78	3.42

In addition to the computations presented for illustration, others were performed and show that the degree of approximation indicated in Table 1 is typical of the model.

## CONCLUSIONS AND RECOMMENDATIONS

A working model has been developed for the analyses of soil-tire interaction. Despite its simplicity, it allows the consideration of the effect of tire deformation on the response of soil. Tire performance calculations based on this model show reasonable agreement with experimental data. The proposed soil-tire model is, therefore, suitable for both performance predictions and parametric design analyses.

In the sample calculations presented, the parameters of tire deformation and the limit normal stress have been selected on the basis of judgment and trial runs with the program. At that time, no attempt was made to establish general relationships that would connect easily measurable tire properties, such as the deflection on rigid surface and inflation pressure, with these parameters. Such relationships, however, can be derived from available experimental data by using the proposed soil-tire model to fit the load torque, drawbar pull, and sinkage data.

Further research is needed for the development of slip-interface friction relationships for tires, with consideration of the slip induced by the hysteresis of the tire material. An analysis of existing tire performance data, using the proposed soil-tire model, would serve as a starting point in this development and at the same time would allow validation of tire deformation characteristics used in the soil-tire model.



## REFERENCES

1. Karafiath, L., "Plasticity Theory and the Stress Distribution Beneath Wheels," Journal of Terramechanics, Vol. 8, No. 2, 1971.
2. Karafiath, L., "On the Effect of Pore Pressures on Soil Wheel Interaction," Proceedings 4th Int. Conf. for Terrain-Vehicle Systems, Stockholm, 1972.
3. Bekker, M., Introduction to Terrain-Vehicle Systems, The University of Michigan Press, 1969.
4. Eberan-Eberhorst, R., "Zur Theories des Luftreifens," ATZ, Vol. 67, No. 8, August 1965.
5. Freitag, D., A Dimensional Analysis of the Performance of Pneumatic Tires on Soft Soils, Technical Report No. 3-688, U.S. Army Engineers Waterways Experiment Station, August 1965.
6. Clark, S., "The Rolling Tire Under Load," SAE Paper No. 650493, May 1965.
7. Dodge, R., "The Dynamic Stiffness of a Pneumatic Tire Model," SAE Paper No. 650491, May 1965.
8. Brewer, H., Stresses and Deformations in Multi-ply Aircraft Tires Subject to Inflation Pressure Loading, Technical Report AFFDL-TR-70-62, June 1970.
9. Freitag, D. and Smith, M., "Center-line Deflection of Pneumatic Tires Moving in Dry Sand," Journal of Terramechanics, Vol. 3, No. 1, 1966.
10. Krick, G., "Radial and Shear Stress Distribution Under Rigid Wheels and Pneumatic Tires Operating on Yielding Soils with Consideration of Tire Deformation," Journal of Terramechanics, Vol. 6, No. 3, 1969.
11. Krick, G., Die Wechselbeziehungen Zwischen Starren Rad, Luftreifen and Nachgiebigem Boden, Dissertation, Technische Universität München, 1971.
12. Stress Under Moving Vehicles, U.S. Army Corps of Engineers Waterways Experiment Station, Technical Report No. 3-545, July 1964.

13. Seitz, N., Experimentelle und Theoretische Untersuchungen der in der Aufstandsfläche frei Rollender Reifen Wirkende Kräfte und Bewegungen, Dissertation, Technische Hochschule München, Clearinghouse Reproduction N69-33739, 1969.
14. VandenBerg, G. and Gill, W., "Pressure Distribution Between a Smooth Tire and Soil," Transactions of ASAE, Paper No. 59-108, 1962.
15. Freitag, D., Green, A., and Murphy, N., "Normal Stresses at the Tire-Soil Interface in Yielding Soils," Highway Research Record, No. 74, 1965.
16. Trabbie, G., Lask, K., and Buchele, W., "Measurement of Soil-Tire Interface Pressures," Agricultural Engineering, November 1959.
17. Bekker, M. and Janosi, Z., Analysis of Towed Pneumatic Tires Moving on Soft Ground, U.S. Army OTAC Report No. RR-6, March 1960.
18. Simon, M., "Les Compacteurs a Pneus en Construction Routiere," Annales de l'Institut Technique du Batiment et des Travaux Public, No. 193, January 1964.
19. Ageikin, Y., "Determination of Ground Contact Parameters in Soft Ground," referenced in Russian Approach to Terrain-Vehicle Systems (M. Bekker), report TR71-30, Delco Electronics General Motors Corp., Santa Barbara, Calif., August 1971.
20. Hovland, H. and Mitchell, J., Mechanics of Rolling Sphere-Soil Slope Interaction, Final Report, Space Sciences Laboratory, University of California, Berkeley, July 1971.